

# Breakdown of the Arrhenius Law of the Temperature Dependent Vacancy Concentration in fcc-Lanthanum

Lucian Mathes, Thomas Gigl, Michael Leitner, and Christoph Hugenschmidt\*  
 Physik-Department E21 and Heinz Maier-Leibnitz Zentrum (MLZ),  
 Technische Universität München, Lichtenbergstraße 1, 85748 Garching, Germany  
 (Dated: August 23, 2021)

We measured the temperature dependent equilibrium vacancy concentration using in-situ positron annihilation spectroscopy in order to determine the enthalpy  $H_f$  and entropy  $S_f$  of vacancy formation in elementary fcc-La. The Arrhenius law applied for the data analysis, however, is shown to fail in explaining the unexpected high values for both  $S_f$  and  $H_f$ : in particular  $S_f = 17(2) k_B$  is one order of magnitude larger compared to other elemental metals, and the experimental value of  $H_f$  is found to be more than three standard deviations off the theoretical one  $H_f = 1.46$  eV (our DFT calculation for La at  $T = 0$  K). A consistent explanation is given beyond the classical Arrhenius approach in terms of a temperature dependence of the vacancy formation entropy with  $S_f^* = -0.0120(14) k_B/K$  accounting for the anharmonic potential introduced by vacancies.

The dominant species of lattice defects, which are thermally created in metal samples, are mono-vacancies. The enthalpy  $H_f$  and entropy  $S_f$  for vacancy formation in thermal equilibrium are key features for the fundamental understanding of physical processes in crystals such as creation of lattice defects and diffusion properties.

There are several experimental techniques where the measured quantity depends on the concentration of (point) defects. Conventionally, measurements of the residual electrical resistivity, which is proportional to the total concentration of all species of lattice defects, are performed to examine the crystal quality or to provide detailed information of defect annealing [1]. Differential dilatometry is sensitive to the volume change associated with the formation of lattice defects in the sample and hence allows the estimation of the vacancy concentration in thermal equilibrium but is limited to temperatures close to the melting point [2]. In contrast, positron annihilation spectroscopy (PAS) is applied as true probing technique to study open-volume crystal defects on an atomic scale. Due to the efficient trapping in the attractive potential formed by vacancies [2, 3] positrons exhibit an outstanding sensitivity for the detection of vacancy concentrations as low as  $c_v \sim 10^{-7}$  [4].

PAS has been widely applied as non-destructive technique to study the annealing behavior [5, 6] and the thermal production of vacancies [7]. The measurement of the equilibrium vacancy concentrations as a function of temperature in turn allows the determination of the vacancy formation enthalpy  $H_f$ . For a large number of elemental metals and alloys the Arrhenius law has been applied in order to obtain values for  $H_f$  and, to lesser extent, for  $S_f$  (see, e.g., [7–10]). Besides specific heat measurements on La providing an estimation of  $H_f = 1$  eV [11], no further data or detailed studies of the vacancy formation in La is reported to best of our knowledge.

In this letter we present measurements of the vacancy concentration in thermal equilibrium in fcc-La up to 1020 K using in-situ PAS. For comparison of the exper-

imental findings with theory we calculated  $H_f$  for La at  $T = 0$  K based on density-functional theory (DFT). For the first data analysis an Arrhenius-like behavior for thermal production of vacancies was assumed, which lead to unexpectedly high values for both the enthalpy  $H_f$  and entropy  $S_f$  for vacancy formation. This discrepancy was attributed to the fact that the formation entropy is mainly affected by the change of the phonon spectrum of the crystal due to the presence of vacancies. In order to obtain a consistent physical explanation we followed a theoretical study by Glensk *et al.* [12] and introduced a temperature dependent vacancy formation entropy.

Lanthanum exhibits phase transitions from dhcp to fcc at  $\sim 560$  K and from fcc to bcc at  $\sim 1120$  K [13]. The melting point of La amounts to 1193 K and its density at room temperature is  $6.145 \text{ g cm}^{-3}$  [14]. The purity of the sample investigated in the present study is  $> 99.9\%$ . Since La is highly reactive and would, e.g., oxidize rapidly when exposed to air, it is kept in ethanol during and after sample preparation. A disc of 4 mm was cut and polished first with SiC grinding paper and subsequently with a  $\text{H}_2\text{O}$ -free diamond suspension with a final grain size of  $1 \mu\text{m}$ . Possible lattice defects have been annealed by heating the sample up to 1020 K with a heating rate of  $13 \text{ K min}^{-1}$  and subsequent adiabatic cooling in the coincident Doppler broadening (CDB) spectrometer prior the temperature dependent measurements. Thus the initial  $S$  parameter of the as-prepared sample at room temperature was reduced by 4%.

Positron-electron annihilation leads predominantly to the emission of two 511 keV  $\gamma$  quanta. These photons, which experience a Doppler shift due to the momentum of the annihilating electrons (the momentum of the thermalized positrons is negligible), are examined by Doppler broadening spectroscopy (DBS) of the positron annihilation line. This broadening strongly depends on the vacancy concentration since the lower annihilation probability of positrons trapped in vacancies with high-momentum core electrons leads to a smaller Doppler-shift

compared to annihilation in the pure lattice. For the characterization of the Doppler broadening the so-called  $S$  parameter is conventionally defined as the fraction of counts in a fixed central region of the annihilation photo peak. Hence, compared to the defect-free state the  $S$  parameter is usually enhanced for positrons trapped in a vacancy. For further details of DBS we refer to [15].

For the present study, we used the CDB spectrometer [16] with a monoenergetic positron beam provided by the neutron induced positron source Munich (NEPOMUC) [17] at the research neutron source Heinz-Maier Leibnitz (FRM II). DBS at this spectrometer with an accessible temperature range of 40 – 1100 K was shown to be particularly suited for the determination of the vacancy concentration, e.g., in Heusler alloys [18] or the in-situ observation of fast defect annealing after severe plastic deformation [19]. In addition, compared to conventional PAS with  $\beta^+$  emitters the usage of a positron beam has the advantage of simple sample heating under ultra high vacuum conditions and that the recorded signal exclusively stems from annihilation events inside the sample (absence of the so-called source component). The kinetic energy of the positron beam can be varied between 0.1 and 30 keV and the spot size of the beam at the sample position is typically 250  $\mu\text{m}$ . In this study a maximum implantation energy of  $E = 28$  keV is used corresponding to a mean positron implantation depth of  $\bar{z} = 1.3$   $\mu\text{m}$  in La. The  $S$  parameter is calculated as the fraction of annihilation events of the photo peak in the energy interval  $(511 \pm 1.7)$  keV. For the determination of the bulk equilibrium vacancy concentration in La at elevated temperature we performed in-situ DBS between 493 and 1023 K in steps of 10 K using the 28 keV positron beam. At each temperature step starting at 1023 K data were recorded for five minutes resulting in about 800 000 counts in the 511 keV annihilation photo peak.

The measured  $S$  parameter as function of temperature is shown in Fig. 1. The total increase of  $S$  from 493 to 1023 K amounts to 7%. Up to temperatures of 700 K a linear rise of the  $S$  parameter is observed with a slope of  $\alpha \approx 2.4(3) \times 10^{-5} \text{ K}^{-1}$ . This linear increase is attributed to the lattice expansion without significant positron trapping in defects and can be very well explained by the thermal volume expansion coefficient of  $\alpha_{\text{th},v} = 3\alpha_{\text{th},l}$ , with  $\alpha_{\text{th},l} \approx 8 \times 10^{-6} \text{ K}^{-1}$  being the thermal linear expansion coefficient of La [20]. This effect correlates to the decreasing overlap of the positron wave function with those of core-electrons being proportional to the volume expansion of the lattice as observed in studies on, e.g., Al, In, and Pb; the effect of a small contraction of the Fermi surface with higher temperature is negligible [21]. It is noteworthy that the phase transition for La at  $\sim 580$  K from dhcp to fcc does not affect the linear slope of the  $S$  parameter or any other of our fit parameters (within the errors) when starting the fit above 600 K. This behavior of  $S(T)$ , however, was ex-

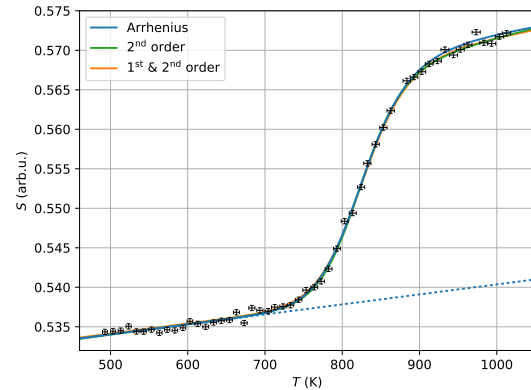


FIG. 1. Measured  $S$  parameter as a function of temperature for La. The experimental data (symbols) are fit by a two-state model for positrons annihilating in the bulk or trapped in vacancies according to Eq. 1 (lines). The linear increase of  $S$  at lower temperature is well described by the thermal lattice expansion (dashed line).

pected since the crystal structures fcc and dhcp differ only in the stacking order. The thermal production of vacancies, which act as efficient positron trapping sites with significantly reduced core annihilation probability, leads to a steeper increase of  $S$  above 700 K according to the equilibrium vacancy concentration at the respective temperature. At about 950 K the  $S$  parameter starts to converge due to so-called saturation trapping, since the high vacancy concentration results in trapping of all positrons.

As first proposed by McKee *et al.* [8], the behavior of the  $S$  parameter can be represented by a superposition of two positron states: positrons annihilate either from a delocalized state in the bulk or from the trapped state in a vacancy with characteristic values  $S_b$  and  $S_v$ , respectively. Hence the  $S$  parameter measured at a given temperature  $S(T)$  can be described by

$$S(T) = \frac{1}{1+Q} S_b(T) + \frac{Q}{1+Q} S_v(T). \quad (1)$$

The temperature dependencies of  $S_b$  and  $S_v$  are considered to be linear in  $T$  with  $(1+\alpha T)$  and  $(1+\beta T)$ , respectively, and well explain the effect of the lattice expansion as discussed. The weighting factors in Eq. 1 are expressed in terms of  $Q$  containing properties of the positron and thermodynamical information

$$Q(T) \equiv \frac{S(T) - S_b(T)}{S_v(T) - S(T)} = \mu \tau_b \cdot c_v(T), \quad (2)$$

with the specific trapping coefficient of a monovacancy  $\mu$ , the bulk lifetime of a positron  $\tau_b$ , and the thermal equilibrium vacancy concentration  $c_v(T)$  at the temperature  $T$ . If not explicitly given,  $\mu \tau_b$  has to be estimated to provide a value for  $c_v$  from the measurements. Since  $\mu \tau_b$  is

actually not known within about one order of magnitude we use the upper limit approximation  $\mu\tau_b \approx 4.4 \times 10^4$  in the following. This value is composed of the trapping coefficient  $\mu = 4 \times 10^{14} \text{ s}^{-1}$  (see, e.g., values for Al [22, 23] and for Cu, Au, Pt [24]), and an assumed positron bulk lifetime in La of  $\tau_b \approx 110 \text{ ps}$ , which is in the range of  $100 \text{ ps} < \tau_b < 120 \text{ ps}$  typically obtained for transition metals (see, e.g., calculated values for the fcc metals Cu, Ag, Ni, and Au [25]).

Assuming monovacancies being the dominant species of lattice defects and in the limit of non-interacting vacancies their concentration is determined by the Gibbs free enthalpy of vacancy formation  $G_f$

$$c_v(T) = \exp(-G_f(T)/k_B T), \quad (3)$$

wherein  $k_B$  is the Boltzmann constant. The temperature dependence of  $G_f$  is conventionally given by

$$G_f(T) = H_f - TS_f, \quad (4)$$

with enthalpy  $H_f$  and entropy  $S_f$  of vacancy formation, both assumed to be temperature-independent. It has to be noted that the respective influence of  $H_f$  and  $S_f$  cannot be separated by any experiment measuring the vacancy concentration. The data shown in Fig. 1 were fitted ('Arrhenius', blue line) by applying Eq. 1 using four parameters ( $S_b^0$ ,  $S_v^0$ ,  $\alpha$  and  $\beta$ ). Tests with different values revealed that any temperature dependence of  $\tau_b$  (see Eq. 2) can be well neglected. By applying Eqs. 3 and 4 this classical model yields a value for the vacancy formation enthalpy of  $H_f = (1.98 \pm 0.15) \text{ eV}$ . Fig. 2 shows the recorded data  $S(T)$  in the common Arrhenius representation where  $H_f$  is given by the linear slope of the data. A linear behavior is observed in the significant region of the covered temperature range. Note that the sensitivity threshold for defect spectroscopy with positrons in the order of  $10^{-7}$  vacancies per atom is clearly visible and saturation trapping starts around  $c_v = 10^{-3}$ .

We computed the vacancy formation energy by DFT with the PBE-generalized gradient approximation [26] using the ABINIT code in the projector-augmented wave framework [27]. We used a plane-wave cutoff of 680 eV and a  $12 \times 12 \times 12$   $k$ -point grid with respect to the conventional cubic unit cell of the fcc lattice. We obtained a lattice constant of 5.29 Å for the ground state, in perfect agreement with the experimental fcc lattice constant extrapolated to zero temperature [28]. The cubic 32 – 1-atom supercell with relaxed internal positions but fixed cell dimensions gave a vacancy formation energy of 1.46 eV, thus perfectly reproducing the previously reported values of 1.44 eV and 1.46 eV [29, 30]. To test for a variation of the formation energy with thermal lattice expansion, we performed additional calculations at a lattice constant of 5.32 Å corresponding to the experimental value around 780 K representative of the temperatures of measurement, which however resulted in only a minute

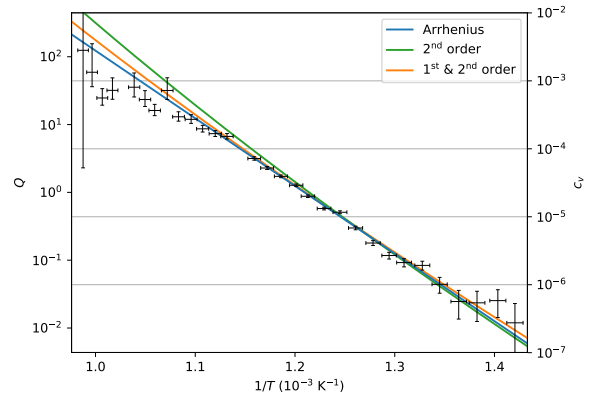


FIG. 2. Arrhenius plot of the measured data. The equilibrium vacancy concentration  $c_v$  (right axis) is deduced from the measured  $Q(T)$  using the approximation  $\mu\tau_b \approx 4.4 \times 10^4$  (see Eq. 2). For the different fits (lines) see text.

increase of the formation energy to 1.50 eV. In order to compare experiment with theory we calculated  $G(T)$  at each temperature from the measured data by combining Eqs. 2 and 3 and the  $S(T)$  fit result (see Fig. 1). Fig. 3 displays the Gibbs free enthalpy as function of temperature with extrapolation of the Arrhenius-fit to  $T = 0 \text{ K}$ . It becomes obvious that the experimental value  $G_f(0) \equiv H_f$  is significantly, i.e., more than three standard deviations, off the calculated one. For the physical interpretation of the data we formally describe the Gibbs free enthalpy in a more general way by applying the Taylor expansion up to the second order

$$G_f(T) \approx G(T_0) + G'(T - T_0) + G''(T - T_0)^2/2 \quad (5)$$

centered at  $T_0 = 850 \text{ K}$ , i.e., at the center of the  $S(T)$  data set;  $G'$  and  $G''$  are first and second partial derivatives, respectively, of the Gibbs free enthalpy with respect to temperature. Two additional fits with fixed  $G_f^{\text{th}}(0) = 1.46 \text{ eV}$  from DFT calculation are performed with and without the linear term (indicated as '1st & 2nd order' and '2nd order') and plotted alongside with the Arrhenius-fit in all Figs. 1 to 3.

The classical Arrhenius law applied to our data for La would yield unrealistic values for both vacancy formation entropy  $S_f$  and Gibbs free enthalpy at  $T = 0 \text{ K}$ . The experimental value of  $G_f(0)$  was found to be 0.52 eV above the calculated one. Hence, the failure of the Arrhenius law becomes apparent in Fig. 3: consequently, the large difference between experimental and theoretical value of  $G_f(0)$  cannot be explained by the conventionally defined Gibbs free enthalpy being linear in temperature. Even more importantly, for the vacancy formation entropy we obtain a lower limit of  $S_f = -\partial G/\partial T = (17 \pm 2) k_B$ ; such high values of  $S_f$  in metals have never been observed to the best of our knowledge. It has to be emphasized that

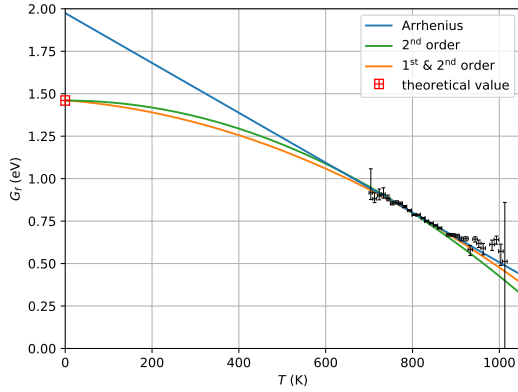


FIG. 3. Gibbs free enthalpy as function of temperature. The different curves correspond to Arrhenius-fit (blue line) as well as fits using the Taylor expansion up to the second order with ‘1<sup>st</sup> & 2<sup>nd</sup> order’ (orange line) and without linear term ‘2<sup>nd</sup> order’ (green line) with the calculated value of  $G_f^{\text{th}}(0) = 1.46$  eV (red symbol) as boundary condition.

this value would correspond to a seven orders of magnitude lower trapping coefficient. Typical  $S_f$  for elemental metals, however, are in the range of  $0.5 - 2 k_B$  [10]; i.e.,  $S_f \approx 1 k_B$  for fcc and  $S_f \approx 2 k_B$  for bcc crystal lattices [31] and hence about one order of magnitude smaller.

The influence of possible divacancies has been proven to be negligible in early experiments [32] and divacancies, e.g., in Al, were shown to be unstable [33]. Theoretical studies yield that the anharmonicity of lattice vibrations are much more significant than the small effect of possible divacancies [34]. This was confirmed in more recent computations of the thermodynamics of divacancies in Al and Cu by Glensk *et al.* [12], who obtained divacancy concentrations  $\leq 4 \times 10^{-3} \cdot c_v$  even at the melting point. The effect of positron detrapping from vacancies was found to somewhat influence the measurements at very high temperature as observed for refractory metals such as Ta [9] but is assumed to be negligible in the temperature range of the present study. According to an empiric description based on a temperature dependent vacancy formation enthalpy Schaefer *et al.* [35] and assuming a ‘real’ formation entropy of  $S_f = 1 k_B$  for La we would obtain a temperature dependence of  $H_f$  of about  $-1.4 \text{ meV/K}^{-1}$ . Besides being purely phenomenological this approach relies on a Gibbs free enthalpy depending linearly on temperature, that in turn is unable to explain the theoretically calculated value of  $G_f^{\text{th}}(0)$ .

In order to describe the exceptionally high  $S_f$  our data can be fitted by using Eq. 5 and the calculated value for  $G_f^{\text{th}}(0)$ . The resulting best fit (with  $G' = 1.53 \times 10^{-3} \text{ eV/K}$  and  $G'' = -7.8 \times 10^{-7} \text{ eV/K}^2$ ) is displayed as ‘1<sup>st</sup> & 2<sup>nd</sup> order’ (orange line) in the figures. It has to be emphasized that this rather formal procedure, i.e., the mathematical description of the Taylor expansion

of  $G(T)$  around 850 K, is intrinsically not able to disentangle information of the temperature dependence of  $H_f$  and  $S_f$ . Therefore, we follow the theoretical approach proposed by Glensk *et al.* [12] who performed demanding finite temperature DFT computations of the Gibbs free energy of vacancy formation by explicitly including anharmonicity due to phonon-phonon interactions, which is of particular importance at high temperatures. Compared to the classical Arrhenius behavior deviations for  $H_f$  of 0.15 and 0.22 eV were found for Al and Cu, respectively [12]. The formation entropy of vacancies was described to be linear in temperature. We now apply this physically justified model (local Grneisen theory) to our experimental results for La and expand  $S_f$  up to the first order in temperature (whereby its constant fraction is neglected as proven to be valid for Al and Cu [12])

$$S_f(T) \approx S'_f T, \quad (6)$$

where  $S'_f$  is the partial temperature derivative of  $S_f$ . Using Eq. 4 we obtain for the Gibbs free enthalpy

$$G_f(T) = H_f^{0K} - T^2 S'_f. \quad (7)$$

Fitting the data hence requires only two free parameters  $H_f^{0K}$  and  $S'_f$ . According to our DFT calculation the first one is found to be  $H_f^{0K} = 1.46$  eV and the second one is  $S'_f = -0.0060(14) k_B/\text{K}$ . The according fit depicted as ‘2<sup>nd</sup> order’ is shown in Figs. 1 to 3. Using this model the linear increase with  $\alpha \approx 2.5(2) \times 10^{-5} \text{ K}^{-1}$  in the temperature range 480 to 700 K is indistinguishable from the other fits as shown in Fig. 1 but clearly deviates from the Arrhenius law at lower temperature (see Fig. 3).

In summary we found unexpectedly high discrepancies for both  $H_f$  and  $S_f$  by applying the classical Arrhenius interpretation to our data obtained by in-situ PAS at high temperatures: the Gibbs free enthalpy at  $T = 0$  K was more than three standard deviations higher than that resulting from our DFT calculation. Even more surprising, however, is the exceptional high value for the entropy  $S_f$ , which was found to be about one order of magnitude higher than typical ones for elemental metal crystals. In this letter, a consistent explanation is given in terms of a temperature dependent vacancy formation entropy taking into account the anharmonicity of phonons introduced by the presence of monovacancies in the crystal lattice.

---

\* [christoph.hugenschmidt@frm2.tum.de](mailto:christoph.hugenschmidt@frm2.tum.de)

- [1] M. Doyama and J. S. Koehler, *Phys. Rev.* **127**, 21 (1962).
- [2] R. Siegel, *J. Nucl. Mater.* **69-70**, 117 (1978).
- [3] C. H. Hodges, *Phys. Rev. Lett.* **25**, 284 (1970).
- [4] P. Hautojärvi, A. Dupasquier, and M. J. Manninen, *Positrons in solids*, Vol. 12 (Springer, 1979).
- [5] S. Mantl and W. Triftshäuser, *Phys. Rev. B* **17**, 1645 (1978).



- [6] M. Eldrup, O. E. Mogensen, and J. H. Evans, *J. Phys. F* **6**, 499 (1976).
- [7] P. Rice-Evans, T. Hlaing, and D. B. Rees, *J. Phys. F* **6**, 1079 (1976).
- [8] B. T. A. McKee, W. Triftshäuser, and A. T. Stewart, *Phys. Rev. Lett.* **28**, 358 (1972).
- [9] K. Maier, H. Metz, D. Herlach, H. E. Schaefer, and A. Seeger, *Phys. Rev. Lett.* **39**, 484 (1977).
- [10] P. Erhart, in *Landolt-Börnstein - Atomic defects in metals*, Vol. Group III Condensed Matter, Vol. 25, edited by H. Ullmaier (Springer Verlag Berlin, Heidelberg, 1991).
- [11] A. I. Akimov and Y. A. Kraftmakher, *Phys. Status Solidi B* **42**, K41 (1970).
- [12] A. Glensk, B. Grabowski, T. Hickel, and J. Neugebauer, *Phys. Rev. X* **4**, 011018 (2014).
- [13] D. A. Young, *Phase diagrams of the elements*, Tech. Rep. (California Univ., 1975).
- [14] L. Gmelin, *Handbuch der anorganischen Chemie*, Vol. 1 (C. Winter, 1886).
- [15] P. Coleman, *Positron beams and their applications* (World Scientific, Singapore, 2000).
- [16] T. Gigl, L. Beddich, M. Dickmann, B. Riencker, M. Thalmayr, S. Vohburger, and C. Hugenschmidt, *New Journal of Physics* **19**, 123007 (2017).
- [17] C. Hugenschmidt, C. Piochacz, M. Reiner, and K. Schreckenbach, *New J. Phys.* **14**, 055027 (2012).
- [18] C. Hugenschmidt, A. Bauer, P. Böni, H. Ceeh, S. W. H. Eijt, T. Gigl, C. Pfeiderer, C. Piochacz, A. Neubauer, M. Reiner, H. Schut, and J. Weber, *Appl. Phys. A* **119**, 997 (2015).
- [19] B. Oberdorfer, E.-M. Steyskal, W. Sprengel, W. Puff, P. Pikart, C. Hugenschmidt, M. Zehetbauer, R. Pippan, and R. Würschum, *Phys. Rev. Lett.* **105**, 146101 (2010).
- [20] F. Barson, S. Legvold, and F. H. Spedding, *Phys. Rev.* **105**, 418 (1957).
- [21] W. Triftshäuser, *Phys. Rev. B* **12**, 4634 (1975).
- [22] H.-E. Schaefer, *Phys. Status Solidi A* **102**, 47 (1987).
- [23] R. Würschum, C. Grupp, and H.-E. Schaefer, *Phys. Rev. Lett.* **75**, 97 (1995).
- [24] H.-E. Schaefer and F. Banhart, *Phys. Status Solidi A* **104**, 263 (1987).
- [25] T. Korhonen, M. J. Puska, and R. M. Nieminen, *Phys. Rev. B* **54**, 15016 (1996).
- [26] J. P. Perdew, K. Burke, and M. Ernzerhof, *Phys. Rev. Lett.* **77**, 3865 (1996).
- [27] X. Gonze, B. Amadon, P.-M. Anglade, J.-M. Beuken, F. Bottin, P. Boulanger, F. Bruneval, D. Caliste, R. Caracas, M. Cote, T. Deutsch, L. Genovese, P. Ghosez, M. Giantomassi, S. Goedecker, D. R. Hamann, P. Hermet, F. Jollet, G. Jomard, S. Leroux, M. Mancini, S. Mazevet, M. J. T. Oliveira, G. Onida, Y. Pouillon, T. Rangel, G.-M. Rignanese, D. Sangalli, R. Shaltaf, M. Torrent, M. J. Verstraete, G. Zerah, and J. W. Zwanziger, *Comput. Phys. Commun.* **180**, 2582 (2009).
- [28] F. H. Spedding, J. J. Hanak, and A. H. Daane, *Journal of the Less Common Metals* **3**, 110 (1961).
- [29] T. Angsten, T. Mayeshiba, H. Wu, and D. Morgan, *New J. Phys.* **16**, 015018 (2014).
- [30] S.-L. Shang, B.-C. Zhou, W. Y. Wang, A. J. Ross, X. L. Liu, Y.-J. Hu, H.-Z. Fang, Y. Wang, and Z.-K. Liu, *Acta Mater.* **109**, 128 (2016).
- [31] K. Maier, M. Peo, B. Saile, H. E. Schaefer, and A. Seeger, *Philosophical Magazine A* **40**, 701 (1979).
- [32] D. Herlach, H. Stoll, W. Trost, H. Metz, T. E. Jackman, K. Maier, H. E. Schaefer, and A. Seeger, *Appl. Phys.* **12**, 59 (1977).
- [33] K. Carling, G. Wahnström, T. R. Mattsson, A. E. Mattsson, N. Sandberg, and G. Grimvall, *Phys. Rev. Lett.* **85**, 3862 (2000).
- [34] N. Sandberg and G. Grimvall, *Phys. Rev. B* **63**, 184109 (2001).
- [35] H.-E. Schaefer, R. Würschum, M. Söb, T. Zák, W. Z. Yu, W. Eckert, and F. Banhart, *Phys. Rev. B* **41**, 11869 (1990).